Analytical and Experimental Investigations for Satellite Antenna Deployment Mechanisms

Masayoshi Misawa* and Tetsuo Yasaka†
NTT Radio Communication Systems Laboratories, Kanagawa, Japan
and
Shojiro Miyake‡
NTT Applied Electronics Laboratories, Tokyo, Japan

This paper deals with the prediction of deployment dynamics, antenna vibration characteristics, and reliability evaluation related with an antenna deployment mechanism (ADM) necessary for large satellite antenna development. A statistical analysis is proposed to predict deployment dynamics of an antenna based on the driving and friction torques of mechanical parts whose statistical distributions are fitted to normal distributions. Test results comprised a range of $\pm\sigma$ (standard deviation) predicted by the analysis. Vibration analysis was performed to clarify the effect of ADM bending stiffness. The effect of ADM bending stiffness on antenna natural frequencies was studied analytically to establish a guideline for determination of the ADM bending stiffness. The first natural frequency of the antenna was lessened by 5 Hz due to the effect of ADM bending stiffness. A procedure is proposed to evaluate the reliability of the ADM. The failure mode and effects analysis was conducted to identify all possible failure modes, among which the critical modes were selected for further investigation. Deployment reliability was calculated assuming that the deployment reliability of the ADM mainly depends on the magnitude of difference between the driving and friction torque.

Introduction

SATELLITE communication systems will require large satellite antennas to realize an economical communication system with large communication capacity.[1] But large satellite antennas for future communication systems raise the serious problem of the shroud diameter limitations of the conventional launch vehicles. Deployable antennas, which will provide a direct solution to the problem, have been extensively studied in recent years.[2-5] Antenna deployment mechanism (ADM) is one of the key technologies in large antenna development for the realization of future economical satellite communication systems.

The main purpose in analyzing the deployment dynamics of an antenna is to select and verify the kinematic properties of the ADM. Several studies[6-9] have been published analyzing detailed dynamic phenomena at small time intervals from initial release to latch up. In these studies, driving and friction torques have been used as definite variables. But in reality, there are variations both in the driving and friction torques.[10] Accordingly, a probabilistic approach for predicting deployment properties is implemented by treating these torques as random variables. The kinematic model is established by considering bearing and latch-pin friction torques, driving torque, and mass properties of the antenna. Latch-up time and velocity, which depend on these parameters, are expanded about the mean of the parameters in a Taylor series. Neglecting higher orders, the expected value and variance of latch-up time and velocity are calculated using the mean and variance of each parameter. The validity of analytical approach is shown by comparing with test results.

Satellite antennas used in the Japanese domestic communication system are required to point the Earth with high accuracy.[1,11] The antennas are vibrated by thruster jets during satellite attitude control and orbit correction maneuvers. Structural deformation due to flexibility represents an unwanted disturbance for the antenna fine pointing. For this reason, it is desirable to make the first natural frequency high in order to keep the deformation small. The bending stiffness of the ADM affects the natural frequencies of the antenna in deployed configuration. Therefore, the effect of the bending stiffness on antenna natural frequencies is investigated to establish a guideline for determination of the ADM component rigidities, which are influential to the bending stiffness. Equations of motion for a system in which an elastic body is supported by a helical spring are based on the assumption that antenna displacements are expressed as the sum of elastic deformations and rigid body displacements. The minimum ADM rigidity is determined from the preceding results and the system dynamic requirements of the spacecraft.

There is, in general, no backup satellite antenna in communication systems due to weight considerations. Therefore, antenna deployment must be accomplished successfully to fulfill the function required by the communication satellite. Reliability evaluation is very important with reference to space mechanical components. A number of papers[12-14] have been published describing the failure analyses and life predictions of mechanical components. But most of them deal with analyses or predictions of mechanical parts, and the rather complex mechanisms such as ADM require a somewhat different approach. A reliability evaluation procedure for the ADM, including selection of test items and reliability prediction, is described in this paper.

ADM Description

The ADM is required to deploy the antenna from the stowed configuration during launch and to lock it precisely in a specified position in orbit. The requirements for strength, resonance frequency, reliability, and weight were taken into account in the ADM design. The ADM consists of two identical hinge mechanisms, each with a spherical bearing, a helical spring, two latch pins, an arm, and a chassis as indicated in Fig. 1. The arm is supported by a shaft through a bearing as shown in Fig. 2. Bearing clearance was chosen carefully to

Received March 7, 1988; presented as Paper 88-2225 at the AIAA/ASME/ASCE/AHS 29th Structural Dynamics, and materials Conference, Williamsburg, VA, April 18-20, 1988; revision received Dec. 6, 1988.

*Senior Research Engineer. Member AIAA.
†Executive Research Engineer. Member AIAA.
‡Senior Research Engineer. Supervisor.

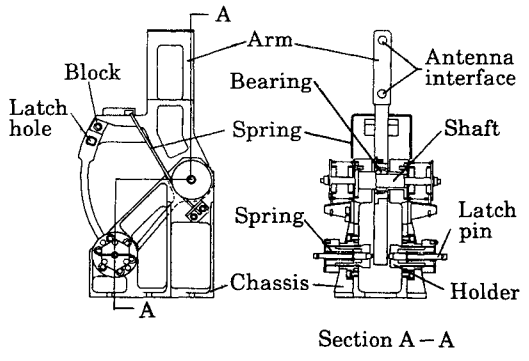

Fig. 1 Hinge mechanism.

maintain high deployment repeatability and to be a positive quantity all the time in the temperature limit requirement of $-90 \sim 105°C$. The titanium bush is interposed to prevent the failure derived from the reduction in bearing clearance and is the best selection in weight reduction. A helical spring provides the driving torque, which is determined so that it ensures full deployment of the antenna and minimizes latch-up load. One end of the spring is fixed to the arm, and the other end of the spring is attached to the chassis. The latch pins and the arc portion of the arm are lubricated with MoS_2 solid lubricant film to minimize friction. The latch pins preloaded by springs are attached to the chassis. During the deployment, the latch pins slide along the arc portion of the arm and are driven into the hole on the arm. To limit the deployment movement in the specified position, blocks were fixed on the arm. These ensure precise locking and prevent the backlash between the arm and chassis in the deployed position. The deployment angle is 1.15 rad.

Deployment Dynamics

Formulation

Antenna deployment is described as a motion about the hinge line of the ADM. The rotational velocity is calculated assuming that the hinge line is fixed in the inertial space, and the antenna is considered a rigid body during the deployment. The undamped equation of motion is given by

$$I\ddot{\theta} + K\theta = T_D - T_F \tag{1}$$

where I is the moment of inertia of an antenna about the hinge line, K the spring constant, θ the deployment angle, T_D the initial driving torque, and T_F the friction torque. Using the initial conditions of the system, $\theta = \dot{\theta} = 0$ at $t = 0$, latch-up time and velocity can be obtained. As the latch-up time and velocity depend on the moment of inertia, the spring constant, and the friction torque, let u denote the latch-up time or velocity and x_1, x_2, x_3 denote the moment of inertia , the spring constant, and the friction torque, respectively. Any or all of these parameters may be random variables. The probabilistic function u is

$$u = u(x_1, x_2, x_3) \tag{2}$$

We expand function u about mean parameters in a Taylor series as

$$u = u_0 + \sum_{i=1}^{3}(x_i - \bar{x}_i)\left(\frac{\partial u}{\partial x_i}\right)_0 + \frac{1}{2}\sum_{i=1}^{3}\sum_{j=1}^{3}(x_i - \bar{x}_i)(x_j - \bar{x}_j)\left(\frac{\partial^2 u}{\partial x_i \partial x_j}\right)_0 + \cdots \tag{3}$$

in which $\bar{x}_i$ is the mean of x_i and subscript 0 shows a value at the mean of each parameter. The expected value of function u

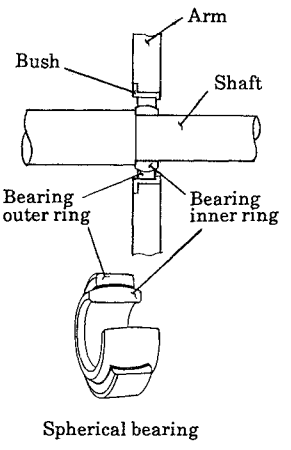

Fig. 2 Connection between arm and shaft.

is given by

$$\bar{u} = \int_{-\infty}^{+\infty}\int_{-\infty}^{+\infty}\int_{-\infty}^{+\infty} u \cdot p(x_1,x_2,x_3)\, dx_1\, dx_2\, dx_3 \tag{4}$$

where p denotes the probabilistic density function of parameters. Substitution of Eq. (3) into Eq. (4) leads to

$$\bar{u} = u_0\int_{-\infty}^{+\infty}\int_{-\infty}^{+\infty}\int_{-\infty}^{+\infty} p(x_1,x_2,x_3)\, dx_1\, dx_2\, dx_3 + \sum_{i=1}^{3}\left(\frac{\partial u}{\partial x_i}\right)_0\int_{-\infty}^{+\infty}\int_{-\infty}^{+\infty}\int_{-\infty}^{+\infty}(x_i - \bar{x}_i)p(x_1,x_2,x_3)\, dx_1\, dx_2\, dx_3 + \frac{1}{2}\sum_{i=1}^{3}\sum_{j=1}^{3}\left(\frac{\partial^2 u}{\partial x_i \partial x_j}\right)_0 \langle x_i,x_j\rangle + \cdots \tag{5}$$

where

$$\langle x_i,x_j\rangle = \int_{-\infty}^{+\infty}\int_{-\infty}^{+\infty}\int_{-\infty}^{+\infty}(x_i - \bar{x}_i)(x_j - \bar{x}_j)p(x_1,x_2,x_3)\, dx_1\, dx_2\, dx_3 \tag{6}$$

The probabilistic density function is expressed as shown in Eq. (7), because random variables considered here are independent of each other:

$$p(x_1,x_2,x_3) = p(x_1)\cdot p(x_2)\cdot p(x_3) \tag{7}$$

Equations (6) and (7) yield the following expression:

$$\langle x_i,x_j\rangle = \begin{cases}\sigma_i^2 & (i = j)\\ 0 & (i \neq j)\end{cases} \tag{8}$$

in which σ_i is a standard deviation of x_i. Neglecting the third- and higher-order terms in Eq. (5), the expected value becomes

$$\bar{u} = u_0 + \frac{1}{2}\sum_{i=1}^{3}\left(\frac{\partial^2 u}{\partial x_i^2}\right)_0\sigma_i^2 \tag{9}$$

The variance of function u is given by

$$\langle u\rangle = \int_{-\infty}^{+\infty}\int_{-\infty}^{+\infty}\int_{-\infty}^{+\infty}(u - \bar{u})^2 p(x_1)\cdot p(x_2)\cdot p(x_3)\, dx_1\, dx_2\, dx_3 \tag{10}$$

It can be also shown that the variance of function u is given by

$$\langle u\rangle = \sum_{i=1}^{3}\left(\frac{\partial u}{\partial x_i}\right)_0^2\sigma_i^2 \tag{11}$$

Equations (9) and (11) show that the expected value and variance can be calculated using the mean and standard deviation of each parameter.

Comparison with Test Results

The driving and friction torques of ADM constituent parts will vary by virtue of manufacturing tolerances, materials variability, and quality control. For example, there is a variation in driving torque, because springs are formed compulsorily with heat treatment in the manufacturing process. Initial driving torque is shown in the measured graphic representation of Fig. 3. Friction torques, caused by bearing and latch pins, are also susceptible to variation as shown in Figs. 4 and 5. These measured data show that the driving and friction torque of the ADM constituent parts are variant and that their distribution can be assumed as normal distributions.

The antenna deployment analysis was accomplished at room temperature both in air and a vacuum. The parameters, indicated in Table 1, were applied to the analysis. The moment of inertia was tentatively considered to be deterministic to make a comparison between the prediction and test, which used a selected model antenna.

The expected value and variance can be calculated using Eqs. (9) and (11) on the assumption that the third- and higher-order terms are neglected in the Taylor series expansion. Thus, it is necessary to check that the higher-order terms are very small. Calculating the ratio of standard deviation to the mean about each parameter, it is found that the third-order terms are very small compared with the second-order ones. Hence, the error in neglecting the higher-order terms is small. The simulated behavior of the latch-up velocity is calculated in Fig. 6. Analytical results are shown in Table 2.

Deployment tests were carried out using an inertia dummy of an antenna to confirm the validity of the statistical approach. An inertia dummy was used so that the effects of air drag during deployment could be kept to a minimum. To minimize the gravity effects, the ADM was mounted to a rigid plate in vertical condition. The prediction and test results on deployment properties are shown in Figs. 7 and 8. The test results comprise a range of $\pm\sigma$ predicted by the preceding analysis. But the standard deviation of the test results is much smaller than the analytical expected value. The reason for the discrepancy is that the number of ADM's is small. Only five sets of ADM's were used to obtain latch-up time and velocity data. Generally, the standard deviation of the test results does not coincide with that of analytical results as long as the amount of test data is small. If we have a great number of test

Table 1 Measured parameters

Parameters	Mean value, μ	Standard deviation, σ
Moment of inertia, N·m·s^2	2.00	0.00
Spring constant, N·m/rad	0.29	0.01
Initial torque, N·m	1.84	0.04
Friction torque, N·m	0.72[a]/0.54[b]	0.06[a]/0.07[b]

[a]Data measured in air. [b]Data measured in vacuum.

Table 2 Analytical results[a]

Item	Mean value, μ		Standard deviation, σ	
	In air	In vacuum	In air	In vacuum
Latch-up time, s	2.15	1.98	0.08	0.07
Latch-up velocity, rad/s	0.94	1.04	0.04	0.04

[a]Deployment angle 1.15 rad.

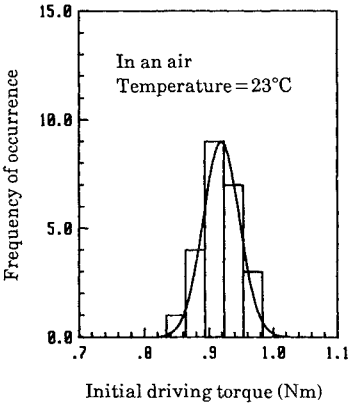

Fig. 3 Initial driving torque distribution (deployment angle: 1.15 rad).

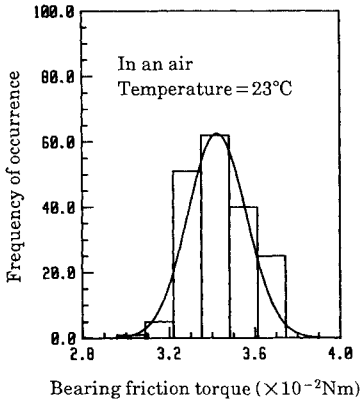

Fig. 4 Distribution of bearing friction torque (radial load: 9.8 N; 1 rpm).

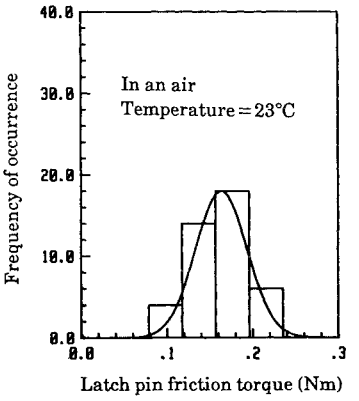

Fig. 5 Distribution of latch-pin friction torque (load: 9.8 N; velocity: 120 mm/s).

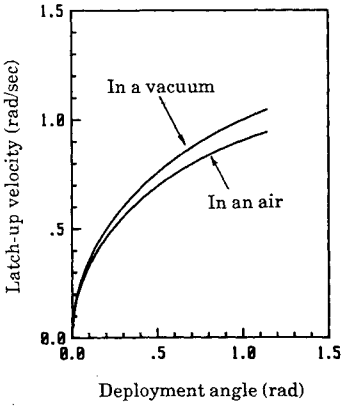

Fig. 6 Simulated behavior of latch-up velocity.

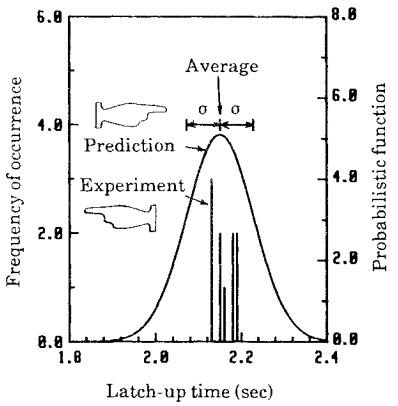

Fig. 7 Measured and predicted latch-up time.

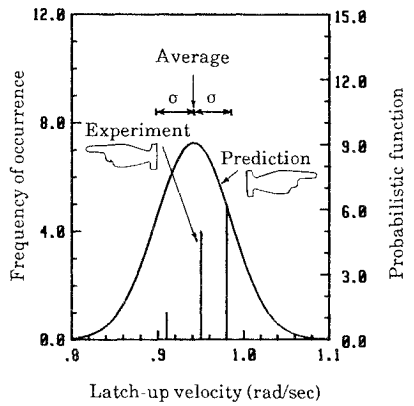

Fig. 8 Measured and predicted latch-up velocity.

data, the standard deviation of the test results will approach the analytical expected value and 99% of the data will be included within a range of $\pm 3\sigma$.

Natural Frequency

Formulation

The bending stiffness of the ADM affects the natural frequencies of the antenna in deployed configuration. The effect of the bending stiffness on antenna natural frequencies was investigated to establish a guideline for determination of the ADM stiffness and associated component wall thicknesses.

Consider a system in which an elastic body is supported by a helical spring as shown in Fig. 9. The undamped equation of motion for the elastic body is

$$[M]\{\ddot{v}\} + [K]\{v\} = \{F\} \tag{12}$$

in which M is a mass matrix, K a stiffness matrix, v a displacement vector, and F a force vector. The displacement vector divided into x and y components can be expressed as

$$\{v\} = \begin{Bmatrix} v_x \\ v_y \end{Bmatrix} \tag{13}$$

The mass matrix is divided in the same way and is assumed to be a diagonal matrix to keep the matter simple. Equations of motion for the system are based on the assumption that antenna displacements are expressed as the sum of elastic deformations and rigid body displacement. The antenna displacements are approximately given by

$$\{v_x\} = \sum_{i=1}^{n} a_i\{v_{xi}\} + \theta\{Y\} \tag{14a}$$

$$\{v_y\} = \sum_{i=1}^{n} a_i\{v_{yi}\} - \theta\{X\} \tag{14b}$$

where X and Y represent the coordinate vector of nodes and n the number of modes. Kinematic energy T and potential energy U are

$$2T = \{\dot{v}_x\}^t[M_x]\{\dot{v}_x\} + \{\dot{v}_y\}^t[M_y]\{\dot{v}_y\} \tag{15a}$$

$$2U = \sum_{i=1}^{n} \omega_i^2 a_i^2 (\{v_{xi}\}^t[M_x]\{v_{xi}\} + \{v_{yi}\}^t[M_y]\{v_{yi}\}) + K_\theta\theta^2 \tag{15b}$$

in which K_θ is a spring constant of the ADM and ω_i the ith angular natural frequency of an elastic body. Substituting Eqs. (14) and (15) into the Lagrange equation,

$$\frac{d}{dt}\left(\frac{\partial T}{\partial \dot{\theta}}\right) - \frac{\partial T}{\partial \theta} + \frac{\partial U}{\partial \theta} = 0 \tag{16a}$$

$$\frac{d}{dt}\left(\frac{\partial T}{\partial \dot{a}_i}\right) - \frac{\partial T}{\partial a_i} + \frac{\partial U}{\partial a_i} = 0 \qquad (i = 1,2,\ldots,n) \tag{16b}$$

the equations of motion are obtained:

$$\begin{aligned} &P_{11}\ddot{a}_1 + (P_{12} - P_{13})\ddot{\theta} + P_{11}\omega_1^2 a_1 = 0 \\ &P_{21}\ddot{a}_2 + (P_{22} - P_{23})\ddot{\theta} + P_{21}\omega_2^2 a_2 = 0 \\ &\qquad\vdots \\ &P_{n1}\ddot{a}_n + (P_{n2} - P_{n3})\ddot{\theta} + P_{n1}\omega_n^2 a_n = 0 \\ &(P_{12} - P_{13})\ddot{a}_1 + \ldots + (P_{n2} - P_{n3})\ddot{a}_n + P_4\ddot{\theta} + K_\theta\theta = 0 \end{aligned} \tag{17}$$

where

$$P_{i1} = \{v_{xi}\}^t[M_x]\{v_{xi}\} + \{v_{yi}\}^t[M_y]\{v_{yi}\} \tag{18a}$$

$$P_{i2} = \{v_{xi}\}^t[M_x]\{Y\} \tag{18b}$$

$$P_{i3} = \{v_{yi}\}^t[M_y]\{X\} \tag{18c}$$

$$P_4 = \{X\}^t[M_x]\{X\} + \{Y\}^t[M_y]\{Y\} \tag{18d}$$

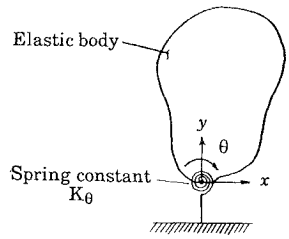

Fig. 9 Analytical model.

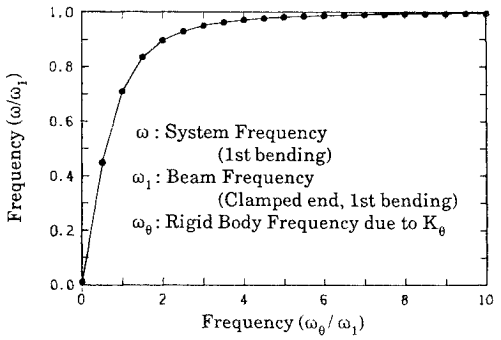

Fig. 10 The first natural frequency including the effect of the ADM bending stiffness.

Numerical Results

An antenna is divided into two parts: a reflector and the ADM. The reflector is an elastic body and the ADM is expressed as a helical spring. To keep the matter simple, a cantilevered beam structure was used in replacement of the reflector. The decrease of the first natural frequency for the

beam was calculated by considering three lower natural frequencies. The analytical result is shown in Fig. 10, in which ω_θ^2 is the ratio of the ADM spring constant to the moment of inertia of the beam about coordinate origin. To satisfy the frequency requirement of the antenna, each requirement for the reflector and ADM is determined from the preceding result by considering the weight needed to make each first natural frequency high.

The bending stiffness of the beam was calculated using force-displacement relation at the tip of the reflector. The first natural frequency of the beam was 7.2 Hz. On the other hand, the spring constant of the ADM was obtained using measured force-displacement relations and was about 1.6×10^4 N · m/rad. In this case, the frequency ratio of ω/ω_1 was 0.35 and the first natural frequency of the antenna was 2.5 Hz. The first natural frequency is lessened by about 5 Hz owing to ADM bending stiffness. This indicates that the additional stiffness increment on the ADM will largely increase the total system bending frequency if a high frequency is still needed by the spacecraft system requirement.

Reliability Evaluation

Problems Associated with Reliability Evaluation

Reliability prediction needs a statistical analysis using probability distributions. Indeed, it has been demonstrated in the area of electronic parts to be feasible and accurate to make such statistical determinations.[15] Electronic parts are standardized and produced in large quantities. Furthermore, failure patterns of mature electronic equipment are reasonably well defined by the easily managed exponential distribution. Therefore, electronic parts readily lend themselves to statistical techniques. On the other hand, many mechanical parts are designed for a particular application and are not standardized. It is difficult to classify such parts with respect to reliability considerations and the assignment of failure rates. These make reliability determination difficult.

A reliability test may be conducted to obtain data necessary for the application to statistical analysis. But many reliability tests of mechanical components are subject to severe realistic restraint, since many parts cannot be tested because of size, cost, or time constraints. Because of a lack of basic reliability data, especially regarding space mechanical components, a realistic evaluation procedure needs careful selection of test items to save money and time.

Procedure of Reliability Evaluation

A flow diagram of reliability evaluation is shown in Fig. 11. First, the ADM was designed to fulfill the previously mentioned requirements. Next, the ADM was classified into several blocks to make a reliability block diagram. The failure mode and effects analysis (FMEA) was conducted considering environmental conditions to identify all possible failure modes, among which the critical modes are selected for further investigation. Finally, deployment reliability was determined using test data.

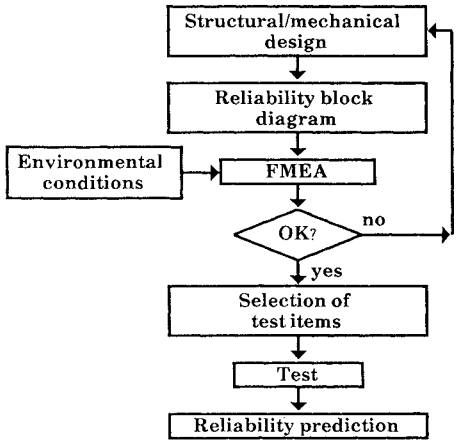

Fig. 11 Flow diagram of ADM reliability evaluation.

Failure Mode and Effects Analysis

Failure modes and their causes were examined considering all the phases from design to operation. An FMEA chart is shown in Table 3. Failure ranks are usually given based on the degree of influence on the antenna system. It is found that failure in every item leads to the fatal function loss in most cases. In the present analysis, the failure ranks were determined on the basis of the failure frequency, the difficulty of failure prevention, and whether the design was new. Rank I is indispensable to design change. Rank II requires design review, and rank III is considered minor. In general, the purpose of FMEA is to take measures to prevent failures by pointing out design deficiencies from the reliability point of view. Because the ranks show the degree of failure related to gravity, they can be considered to give priority in selecting test items. Thus, the items indicated by rank II were selected for further investigation in evaluating the reliability of the ADM. The bearing performance and friction are critical, and detailed tests performed.

Failure Modes

Thermal stress is a serious problem because it causes the variation of bearing clearance. An example of deployment malfunction is shown in Fig. 12. The deployment angles attained after release mechanism initiation are plotted against the environmental temperature. Deployment sequence did not begin at the temperature of $-90°C$, and the deployment was accomplished fully at a temperature of about $-60°C$. As a result of clearance measurements on bearings in the identical lot, it was found that the bearing clearances were distributed in a wide range as indicated in Fig. 13 and that a considerable number of bearings had smaller clearances than the catalog data. The difference of thermal expansion ratio among the arm, bearing, and shaft caused the contraction of the arm, and this reduced the bearing clearance. Hence, titanium bush was interposed between the arm and bearing so that no excessive force could be applied to the bearing in the temperature range of -90–$150°C$ to prevent failures derived from the reduction in bearing clearance. The change of bearing clearance due to the contraction of the arm is given by

$$\Delta = \frac{2m\delta}{(m^2-1)\left\{\dfrac{m^2+1}{m^2-1} - \nu_1 + \dfrac{E_1}{E_2}\left[\dfrac{n^2+1}{n^2-1} + \nu_2\right]\right\}} \tag{19}$$

where $m = b/c$ and $n = a/b$.

In Eq. (19), a is the outer diameter (o.d.) of the bush, b the o.d. of the bearing, c the inner diameter of the bearing, δ the interference between the bush and the bearing outer ring, E Young's modulus, ν Poisson's ratio, and subscripts 1 and 2 show the quantities related to the bearing and the bush. It is found that the titanium bush effectively lessens the change of bearing clearance.

It is absolutely necessary to understand lubricant characteristics, because there is quite a possibility that a change of the characteristics interrupts the antenna deployment. The tests on parts are more advisable than those on the assembled from the standpoint of cost saving. Still, since characteristics of parts may not represent the characteristic of the parts actually used in the mechanism, the tests of a few mechanisms are actually required. Therefore, it is very important to establish the evaluation method of lubricated parts by seeing part characteristics in relation to ADM characteristics. A procedure is shown in Fig. 14. Because the difference in part test conditions and environmental conditions (ADM test conditions) causes the disagreement between two characteristics, part test conditions were improved by inspecting the sliding surface and friction coefficient in two conditions. After we confirmed that the sliding surfaces on parts themselves and those inserted into

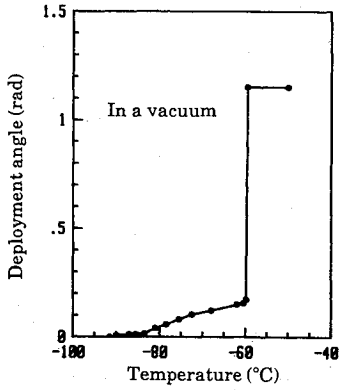

Fig. 12 Behavior of the deployment angle.

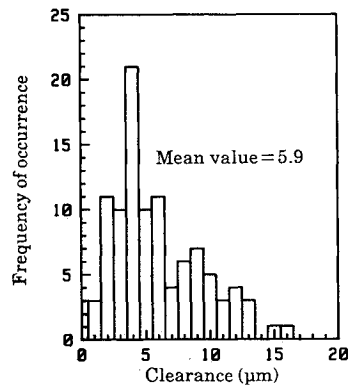

Fig. 13 Bearing clearance.

the ADM suffered a similar damage, we continued to acquire part data. An example of latch-pin friction characteristics is shown in Fig. 15. Friction coefficients both in a vacuum and in air that are initially about 0.2 start to increase after a few thousand cycles. The friction coefficient in a vacuum is noted to be smaller than that in air. The latch pin will have enough endurance life when one considers the actual latch-pin operation cycles both before and after the satellite launch.

Deployment Reliability

The probability of failure concerning mechanical parts such as springs, sliders, and bearings is very small during the mission life. Because the ADM is used only once, it is not always effective to perform a life test of the parts. It is proper that deployment reliability is considered to be determined by part characteristics, because deployment dynamics depends on those characteristics. Assuming that the deployment reliability of the ADM mainly depends on the magnitude of the difference between the driving and friction torques, the deployment reliability is defined as

$$R = \text{prob}\,(X > Y) \tag{20}$$

in which X is the driving torque and Y the friction torque. Since the driving and friction torques of ADM constituent parts are fitted to normal distribution as previously stated, these torques of the ADM can be also fitted to normal distribution. Deployment reliability is easily obtained by computa-

Table 3 Failure mode and effects analysis of the antenna deployment mechanism

Assemblies	Items	Failure modes	Causes	Influences on system	Failure rank
Chassis assembly	Chassis	Break/damage	Dynamic and static load	Unfulfillment of communication system	III
		Deformation	Temperature change Dynamic and static load	Drop in electrical performance	III
Shaft assembly	Shaft	Damage	Dynamic and static load	Drop in electrical performance	III
		Deformation	Dynamic and static load	Drop in electrical performance	III
	Bearing	Reduction in clearance	Temperature change	Unfulfillment of communication system	II
		Increase in clearance	Temperature change	Drop in electrical performance	III
		Break/damage	Dynamic and static load Faulty fitting	Unfulfillment of communication system	III
		Deformation	Dynamic and static load Faulty fitting	Drop in electrical performance	III
	Lubricant	Peeling	Slide Inadequate lubrication	Unfulfillment of communication system	II
		Increase in friction torque	Temperature change Pressure change	Unfulfillment of communication system	II
		Contamination	Dust	Unfulfillment of communication system	III
Latch-pin assembly	Latch-pin	Damage	Shock load	Drop in electrical performance	III
	Spring	Decrease in load	Temperature change	Drop in electrical performance	III
Arm assembly	Arm	Break/damage	Dynamic and static load	Unfulfillment of communication system	III
		Deformation	Dynamic and static load	Drop in electrical performance	III
	Driving spring	Drop in driving torque	Temperature change	Unfulfillment of communication system	II
	Lubricant	Peeling	Slide Inadequate lubrication	Unfulfillment of communication system	II
		Increase in friction coefficient	Temperature change Pressure change	Unfulfillment of communication system	II
		Contamination	Dust	Unfulfillment of communication system	III
	Block	Deformation	Temperature change	Drop in electrical performance	III
Connecting parts	Bolt, nut, screw	Looseness	Dynamic and static load	Drop in electrical performance	III
		Damage	Dynamic and static load	Drop in electrical performance	III

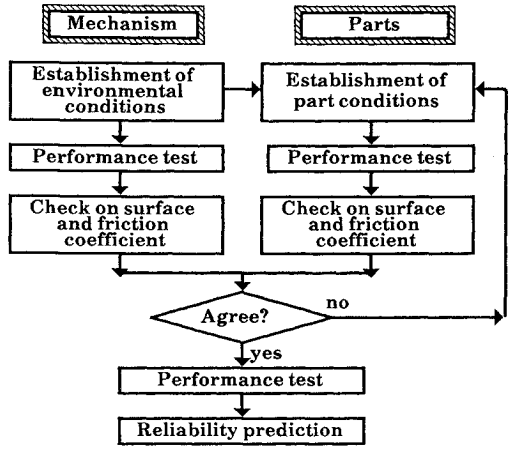

Fig. 14 Flow diagram of lubricated part evaluation.

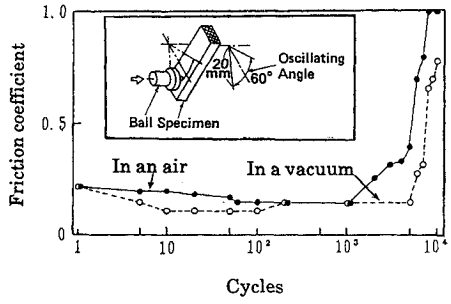

Fig. 15 Sliding endurance life of latch pin (load: 9.8 N; velocity: 120 mm/s).

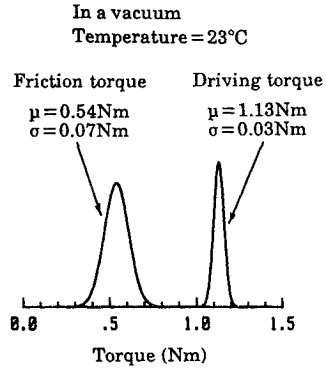

Fig. 16 Torque distribution of the ADM.

tion using the measured data. The example shown in Fig. 16 yielded the reliability of $0.9_{12}5$. The reliability of the ADM subsystem is the product of this failure and the structural reliability. The actual reliability target will be determined considering the total system reliability requirement, weight, and cost.

A very high reliability can be derived even under a very conservative assumption as defined in Eq. (20) using the component data obtained in a limited number of selected test items. This evaluation procedure may be justified by the fact that the reliability of a mechanical system that operates only once is demonstrated avoiding very costly system tests that will require a substantial number of identical mechanisms.

Conclusion

An analytical study was performed to predict deployment dynamics of an antenna based on the fact that the driving and friction torques of the ADM constituent parts fit the normal distribution. The expected value and variance of latch-up time and velocity were calculated using the mean and standard deviation of each part distribution. The analytical approach is confirmed to be valid from the test results, which comprised a range of $\pm\sigma$ predicted by the analysis.

The effect of ADM bending stiffness on antenna natural frequencies was studied analytically to establish a guideline for determination of the ADM bending stiffness. Equations of motion for a system in which an elastic body is supported by a helical spring were led on the assumption that the displacements of the antenna are expressed as the sum of elastic deformations and rigid body displacement.

A procedure was proposed to evaluate the reliability of the ADM. An FMEA was conducted to identify all possible failure modes. In this analysis, failure ranks were determined on the basis of the degree of influence on the antenna system, the failure frequency, the difficulty of failure prevention, and so on. Critical failure modes from FMEA were found to be the bearing performance and friction torque. Assuming that the deployment failure mainly depends on the magnitude of the difference between the driving and friction torques, the deployment reliability was computed based on these distributions. The procedure proposed in this paper is a realistic and reasonable evaluation method for a mechanical component.

References

[1]Yasaka, T., Ohtomo, I., Minimo, M., Kumazawa, H., and Kawakami, Y., "Multi-band Multi-beam Antenna Complex for Orbit Experiment," International Astronautical Federation Paper IAF-87-488, 1987.

[2]Bush, H. G. and Heard, W. L., Jr., "Recent Advances in Structural Technology for Large Deployable and Erectable Spacecraft," International Astronautical Federation Paper IAF-80-A-27, 1980.

[3]Russell, R. A., Campbell, T. G., and Freeland, R. E., "A Technology Development Program for Large Space Antennas," International Astronautical Federation Paper IAF-80-A-33, 1980.

[4]Watanabe, M., Misawa, M., Minomo, M., and Yasaka, T., "High Accuracy Deployable Antenna for Communications Satellite," *Proceedings of the 13th International Symposium on Space Technology and Science,* Organized Committee of the 13th ISTS, Tokyo, 1982.

[5]Misawa, M., Kumazawa, H., and Minimo, M., "Configuration and Performance of 30/20 GHz Band Shaped-beam Antenna for Satellite Use," AIAA Paper 84-0868, May 1984.

[6]Martin, K. and De'Ath, D., "Evolution from Hinge Actuator Mechanism to an Antenna Deployment Mechanism for Use on the European Large Communications Satellite (L-SAT/OLYMPUS)," *Proceedings of the 18th Aerospace Mechanism Symposium,* NASA, Scientific and Technical Information Branch, 1984, pp. 79-91.

[7]Stella, D., Morgant, F., and Nielsen, G., "Contraves' Antenna Tip Hinge Mechanism for Selenia Spazio's 20/30 GHz Antenna," *Proceedings of the 2nd ESA Workshop on Mechanical Technology for Antennas,* European Space Agency, Paris, 1986, pp. 185-194.

[8]James, P. K., "Simulation of Deployment Dynamics for INTELSAT VI Transmit and Receive Boom/Antenna Systems," *COMSAT Technical Review,* Vol. 15, No. 1, 1985.

[9]White C., and Todd, M. J., "Torque Properties of Oscillating Dry-Lubricated Ball Bearings in Vacuum," European Space Agency, Paris, Contract ESTEC 4099/79/NI, 1984, p. 4305.

[10]Misawa, M., Miyake S., and Yasaka, T., "Reliability Evaluation on On-Board Satellite Antenna Mechanism," *Journal of the Japanese Society for Aeronautical and Space Sciences,* Vol. 36, March 1988.

[11]Kawakami, Y., Kumazawa, H., Ohtomo, I., Minomo, M., and Yamada Y., "On-board Ka-band Multibeam Antenna System with High Pointing Accuracy for ETS-VI," GLOBECOM, 1987, Institute of Electrical and Electronics Engineers, New York, pp. 24.8.1-24.8.5.

[12]Dutton, G. Stoy, "Reliability Analysis of Non-Electronic Component Using Weibull, Gamma and Log Normal Distributions," U.S. Air Force Institute of Technology, GRE/MATH/64-12, 1964.

[13]Weaver, I. A. and Smith, M. P., "The Life Distribution and Reliability of Electro-mechanical Parts of an Inertial Guidance System," *Proceedings of the 8th National Symposium on Reliability and Quality Control,* 1962.

[14]Donald, W. F. and Fulton, W., "The Reliability analysis of Nonelectronic Components," Applied Research Lab., RAS-TM-63-2, 1963.

[15]"Reliability Prediction of Electronic Equipment," U.S. Department of Defense, MIL-HDBK-217B, 1974.